Monthly Notices
of the
ROYAL ASTRONOMICAL SOCIETY

MNRAS **450,** 956–966 (2015) doi:10.1093/mnras/stv661

Oscillations in stellar superflares

L. A. Balona,[1⋆] A.-M. Broomhall,[2,3] A. Kosovichev,[4] V. M. Nakariakov,[2,5] C. E. Pugh[2] and T. Van Doorsselaere[6]

[1]*South African Astronomical Observatory, PO Box 9, Observatory 7935, South Africa*
[2]*Centre for Fusion, Space and Astrophysics, Department of Physics, University of Warwick, CV4 7AL, UK*
[3]*Institute of Advanced Studies, University of Warwick, Coventry CV4 7HS, UK*
[4]*New Jersey Institute of Technology, Newark, NJ 07103, USA*
[5]*Central Astronomical Observatory at Pulkovo of the Russian Academy of Sciences, St Petersburg 196140, Russia*
[6]*Centre for mathematical Plasma Astrophysics, Department of Mathematics, KU Leuven, Celestijnenlaan 200B bus 2400, B-3001 Leuven, Belgium*

Accepted 2015 March 24. Received 2015 March 24; in original form 2015 February 6

ABSTRACT

Two different mechanisms may act to induce quasi-periodic pulsations (QPP) in whole-disc observations of stellar flares. One mechanism may be magnetohydromagnetic forces and other processes acting on flare loops as seen in the Sun. The other mechanism may be forced local acoustic oscillations due to the high-energy particle impulse generated by the flare (known as 'sunquakes' in the Sun). We analyse short-cadence *Kepler* data of 257 flares in 75 stars to search for QPP in the flare decay branch or post-flare oscillations which may be attributed to either of these two mechanisms. About 18 per cent of stellar flares show a distinct bump in the flare decay branch of unknown origin. The bump does not seem to be a highly damped global oscillation because the periods of the bumps derived from wavelet analysis do not correlate with any stellar parameter. We detected damped oscillations covering several cycles (QPP), in seven flares on five stars. The periods of these oscillations also do not correlate with any stellar parameter, suggesting that these may be a due to flare loop oscillations. We searched for forced global oscillations which might result after a strong flare. To this end, we investigated the behaviour of the amplitudes of solar-like oscillations in eight stars before and after a flare. However, no clear amplitude change could be detected. We also analysed the amplitudes of the self-excited pulsations in two δ Scuti stars and one γ Doradus star before and after a flare. Again, no clear amplitude changes were found. Our conclusions are that a new process needs to be found to explain the high incidence of bumps in stellar flare light curves, that flare loop oscillations may have been detected in a few stars and that no conclusive evidence exists as yet for flare induced global acoustic oscillations (starquakes).

Key words: stars: activity – stars: flare.

1 INTRODUCTION

Photometric observations from the *Kepler* spacecraft have revealed flares in a considerable number of stars. These occur not only in cool M dwarfs, but in K, G, F and A stars as well. The numbers of B stars observed by *Kepler* are too few to allow detection of flares. Because even the weakest visible stellar flares are thousands of times more energetic than a large solar flare, these are often called 'superflares'. Walkowicz et al. (2011) were the first to identify 373 flare stars out of ≈23 000 cool dwarfs in the *Kepler* field. Subsequently, Maehara et al. (2012) discovered 148 solar-type stars with superflares. More recently, Shibayama et al. (2013) found superflares on 279 G dwarfs. Balona (2012, 2013) discovered several A stars with superflares which cannot be attributed to flares in a cool companion. It appears that A stars may have spots and flares in spite of the lack of significant convection. In fact, the incidence of flares on A stars is not much lower than in G and F stars (Balona 2015). In these hot stars the magnetic field may be a result of the Tayler instability in a differentially rotating star (Spruit 2002; Mullan & MacDonald 2005).

Whereas solar flares emit predominantly in several discrete chromospheric and UV lines of highly ionized elements, the optical flux in stellar flares appears to be distributed much like the continuum of an A or B star (Kowalski et al. 2013). White-light emission in solar flares is difficult to detect, though it is possible that it might contribute a large fraction of the total flare radiation (Kretzschmar 2011). Even the strongest solar flares are barely detected in space

⋆ E-mail: lab@saao.ac.za

observations of total solar irradiance and the Sun would not be detected as a flare star by *Kepler*. It is thought that solar flares arise from the energy released by magnetic reconnection. Although superflares are typically 10^6 times more energetic than large solar flares, it is possible that the magnetic reconnection model may still apply (Shibata et al. 2013).

Nearly all *Kepler* photometry has been obtained with 30-min long-cadence (LC) exposures, which means that only flares which have a long duration can be detected. A few thousand stars were observed with 1-min short-cadence (SC) exposures, though only for a relatively short time. Whereas LC data are nearly continuous over the four-year time span of *Kepler* observations, the SC data cover typically only a few months for any star. The advantage of SC data is that they allow flares of short duration to be detected. Balona (2015) discovered 3140 flares in 209 stars of all spectral types observed in SC mode. In this paper, the flare in a particular star is identified by its sequence number. For example 002300039-028 is the 28th flare in KIC 2300039 listed in the catalogue of Balona (2015).

We know that quasi-periodic pulsations (QPP) of coronal loops occur in some solar flares (Nakariakov & Melnikov 2009; Nakariakov et al. 2010). The mechanism giving rise to QPP is not fully understood at present. One possibility pointed out by McLaughlin, Thurgood & MacTaggart (2012) is that of oscillatory reconnection. The behaviour of oscillatory reconnection is similar to a damped harmonic oscillator and may play a role in generating QPP.

Analysis of QPP can provide information on the flare coronal environment and magnetic field strength by the use of seismology (Kupriyanova, Melnikov & Shibasaki 2013). However, solar flare QPP are only observed in Hα, extreme UV lines and in radio and X-ray and gamma-ray observations. There are no recorded observations of QPP in white-light solar flares. The reported optical observations of QPP in stellar flares (Rodono 1974; Zhilyaev et al. 2000; Mathioudakis et al. 2006; Contadakis, Avgoloupis & Seiradakis 2010; Qian et al. 2012; Anfinogentov et al. 2013), which have periods ranging from a few seconds to tens of minutes, are whole-disc essentially white-light observations. They cannot therefore be directly compared with solar flare QPP. It is also far from certain if white-light stellar flares are generated in the same way as solar flares.

Solar and stellar QPP have previously been used to provide estimates for several flare parameters. An example of QPP with large amplitude and duration in a solar flare observed in X-ray and microwave radio bursts is described by Kane et al. (1983). More recently, Van Doorsselaere et al. (2011) used X-ray observations of two oscillation modes in a single solar flare to estimate the plasma-beta and the density contrast of the flaring loop. The wavemode number was also estimated from the observed periods. Anfinogentov et al. (2013) analysed the oscillatory signal in the decay phase of the *U*-band light curve of a flare in the dM4.5e star YZ CMi. The observational signature is typical of the longitudinal oscillations observed in solar flares at extreme UV and radio wavelengths and is associated with standing slow magnetoacoustic waves. They therefore suggest that the QPP in this stellar superflare may be of a similar nature to solar QPP. A well-pronounced QPP has been reported during a very energetic flare on the RS CVn binary II Peg (Mathioudakis et al. 2003). The QPP has a long period leading to the peak.

The dynamic impact in the photosphere caused by a solar flare is called a 'sunquake'. The resulting helioseismic waves are observed as expanding circular ripples on the solar surface, which can be detected in Dopplergrams and as a characteristic ridge in time–distance diagrams (Kosovichev & Zharkova 1998; Kosovichev 2006), or by calculating the integrated acoustic emission (Donea, Braun & Lindsey 1999; Donea & Lindsey 2005). These flare-excited oscillations are mostly local seismic waves. While the theory predicts that global acoustic waves should also be excited, their amplitudes are thought to be significantly lower than the amplitudes of stochastically excited oscillations (Kosovichev 2009). Most of the emitted acoustic energy of sunquakes is above the acoustic cut-off frequency of the Sun.

Karoff & Kjeldsen (2008) concluded that global high-frequency solar acoustic waves have larger amplitudes after some solar flares, a finding confirmed by Kumar et al. (2010). However, Richardson, Hill & Stassun (2012) found that a decrease in acoustic power after a solar flare is just as likely as an increase. This is perhaps not surprising because the effect of the impulse on a global seismic mode depends on the location and time of the impulse. The effect of the impulse is therefore expected to increase the amplitude of some modes and decrease the amplitude in other modes. The result should be a higher variation in amplitude distribution after a flare.

In the case of the vastly more powerful stellar superflares, the impact on the star may be much greater and it is conceivable that these forced oscillations may be observed. This idea has been discussed by Karoff (2014) and Kosovichev (2014) in *Kepler* photometry of solar-like stars. Karoff found no significant enhancement of the energy in the post-flare acoustic spectra relative to the pre-flare energy. However, a larger variability between the energy in the high-frequency part of the post- and pre-flare acoustic spectra was found compared to spectra taken at random times. This may be a result of the increased dispersion in acoustic energy discussed above.

In spite of the very large differences in energy and optical emission between solar and stellar flares, the possibility exists that the physical mechanisms for QPP could be very similar. In this paper, we investigate QPP in *Kepler* superflares because this could provide additional clues to the nature of stellar flares. We also investigate the possible occurrence of starquakes as a result of a superflare and search for excitation of global acoustic oscillation modes in the periodogram. These investigations are only possible due to the superb precision of the *Kepler* data, a unique resource which is unlikely to be equalled for many years to come.

2 DATA AND ANALYSIS TECHNIQUE

Our analysis is based on the 3140 flares in 290 stars observed in SC mode as described in Balona (2015). Out of these 3140 flares, we selected 257 flares in 75 stars with sufficiently high signal-to-noise (S/N) to be suitable for detecting possible flare oscillations.

In order to enhance the visibility of possible oscillations it is necessary to remove the underlying flare decay. We found that a polynomial of the form

$$\log(y) = a_0 + a_1 t + a_2 t^2 + a_3 t^3 \cdots$$

generally provides a good fit to the flare decay intensity. Here, t is the time measured from flare maximum and y is the flare intensity. In nearly every case, a cubic polynomial was used. The polynomial was removed and the residuals plotted as a function of time. In about 18 per cent of the *Kepler* flares, one or more bumps are present in the decay branch. A low-degree polynomial does not adequately remove these features. In these cases, the large-scale structures can be removed by applying a suitable filter to the data, as described below.

Flare loop oscillations (QPP) are usually seen as damped sinusoidal oscillations (there are however decay-less, multimodal and

wavetrain regimes observed). Wavelet analysis is an appropriate tool for detecting such a signal. Wavelet analysis decomposes a time series into time/frequency space simultaneously. One gets information on both the amplitude of any periodic signals within the series, and how this amplitude varies with time. This is accomplished by selecting an appropriate wavelet function that can be scaled and translated. The resulting wavelet transform is a representation of the signal at different time-scales. We use the Morlet wavelet (a sine wave multiplied by a Gaussian envelope) as the basis function in our analysis. The results are shown in a plot of instantaneous waveperiod and amplitude as a function of time. This is conveniently accomplished by a grey-scale representation of the amplitude in a period–time diagram.

Forced global acoustic oscillations caused by a flare impulse are expected to be seen several hours after the flare and with a decay time of perhaps a few days. For detecting such oscillations we use standard periodogram analysis applied to a data window with a length of a few days and starting a few hours after the flare.

3 FLARES WITH BUMPS IN THE LIGHT CURVE

Of 257 stellar flares selected because of their very high S/N, 47 flares (i.e. 18 per cent) show obvious structures (i.e. bumps) in the flare decay light curve. A further 14 per cent show a distinct change in the rate of decay (Balona 2015). Examples of flare light curves showing bumps are shown in Fig. 1. One possible reason for such bumps is that two flares occur by chance within the same small interval. One can estimate the chances of such an occurrence by measuring the mean flare rate during a suitable interval. The typical duration of a flare is about one hour. The star with the maximum flare rate produces, on average, one flare every 10 h or $x = 0.1$ flare h^{-1}. The probability, P, that two flares will occur in the interval of one hour follows a Poisson distribution and is $P = \frac{x^2}{2!}\mathrm{e}^{-x} = 0.005$. This is an upper limit considering the fact that we have chosen the maximum flare rate. In some stars (e.g. KIC 11551430) there are many flares with bumps. The probability of such an occurrence, assuming that what we are seeing is just a superposition of two or more practically simultaneous flares, is negligible. Hence there must be a physical process involved in producing the bumps. One such process could be sympathetic flaring where one solar flare may trigger another flare (Moon et al. 2002).

Both bumps and changes in rate of decay can be modelled as QPP with a rapid decay rate. In Fig. 1, the polynomial fit to the decaying branch, and the wavelet spectra are shown. Wavelet analysis of 47 'bump' flares in 30 stars indicates that significant power is present at a certain period. If we are to make progress in understanding this relatively common phenomenon, the 'period' derived in this may offer some clue as to the nature of the bumps.

If we assume that the bump is due to a highly damped global acoustic mode, for example, one may expect the period to be correlated with some stellar parameter or combination of parameters. Solar-like modes in stars are excited because their periods are similar to the typical turn-over period of a convective cell and below the acoustic cut-off frequency. As a result, the frequency of maximum amplitude, $\nu_{\max}$ is related to the stellar parameters as follows (Brown et al. 1991; Kjeldsen & Bedding 1995):

$$\nu_{\max} \approx \nu_{\max\odot}\frac{M/\mathrm{M}_\odot}{(R/\mathrm{R}_\odot)^2\sqrt{T_{\rm eff}/\mathrm{T}_{\rm eff\odot}}},$$

where the solar value for the frequency of maximum amplitude is $\nu_{\max\odot} = 3120$ μHz, while $M/\mathrm{M}_\odot$, $R/\mathrm{R}_\odot$ and $T_{\rm eff}/\mathrm{T}_{\rm eff\odot}$ is the stellar mass, radius and effective temperature relative to the Sun.

If, by analogy with sunquakes, the stellar flares excite mostly acoustic modes with frequencies close to the acoustic cut-off frequency, one might expect a correlation between the period and the acoustic cut-off frequency. Since the acoustic cut-off frequency is proportional to $\nu_{\max}$, one may expect a correlation between the bump period and $P_{\max} = 1/\nu_{\max}$. The value of $P_{\max}$, as calculated from $\log g$ and $T_{\rm eff}$, is shown in Table 1.

As shown in Table 2, the flare bump period ($P_{\rm bump}$) can vary widely even in the same star. We can find no correlation between this period and $P_{\max}$. In fact, no correlation between these time-scales and any stellar parameter can be found. It seems that the structures on the decaying branch of the flare, whatever their cause, cannot be attributed to highly damped impulsively excited global acoustic oscillations. It is still possible that these may be highly damped flare loop oscillations, but there is no evidence that can be used in support of this notion either. However, the similarity of the observed decaying QPP in stellar superflares, and of the standing oscillations observed in hot coronal solar flare loops (e.g. Wang 2011; Kim, Nakariakov & Shibasaki 2012) indicates the possible similarity of the physical processes involved, despite differences in emission spectrum.

4 RAPID OSCILLATIONS

A polynomial fit to the flare decay branch is no longer adequate to enhance the visibility of possible oscillations with periods of only a few minutes. We found a segmented spline fit to be adequate for this purpose. In this method, a number of evenly spaced points are selected in the decay branch of the flare light curve. The mean intensity in the neighbourhood of each point is found. A spline fit is calculated using the time and mean intensities at these points and the fit removed from the data. It is important to choose the interval between the segments carefully. If the interval is too small, possible oscillations with periods longer than this interval will not be detected because less than one period will be sampled. On the other hand, if the interval is too long, then the spline interpolation is no longer an adequate fit and the residuals may be contaminated by spurious long-period signals. We found that a choice of 10–15 min was appropriate for the interpolation sampling interval in most cases. We have also tried other methods for trend removal, such as temporal smoothing, but this did not significantly influence the detected periods.

We carefully examined all 257 flares without finding any obvious QPP in the majority of flares. We did not find any cases where QPP begins before the time of flare maximum. This may be due to the long sample time of 1 min and the steep rising branch which would make such a detection difficult. Evidence for damped oscillations after flare maximum is, however, present in the few flares shown in Figs 2–8. The stellar parameters for these stars are shown in Table 2. Most of these flares also appear in Table 1; other stars in this table do not show more than a single bump.

Gruber et al. (2011) tested the apparent QPP of four bright solar flares observed in gamma rays using classical periodogram analysis, but found that these oscillations were not intrinsic to the flares. Similarly, Vaughan (2010) applied Bayesian statistics to apparent QPP in some Seyfert galaxies and also found that these were not significant. The difficulty is that the underlying noise in the periodogram is not 'white' (i.e. independent of frequency) but 'red' (i.e. increases towards low frequencies). This variation of noise with

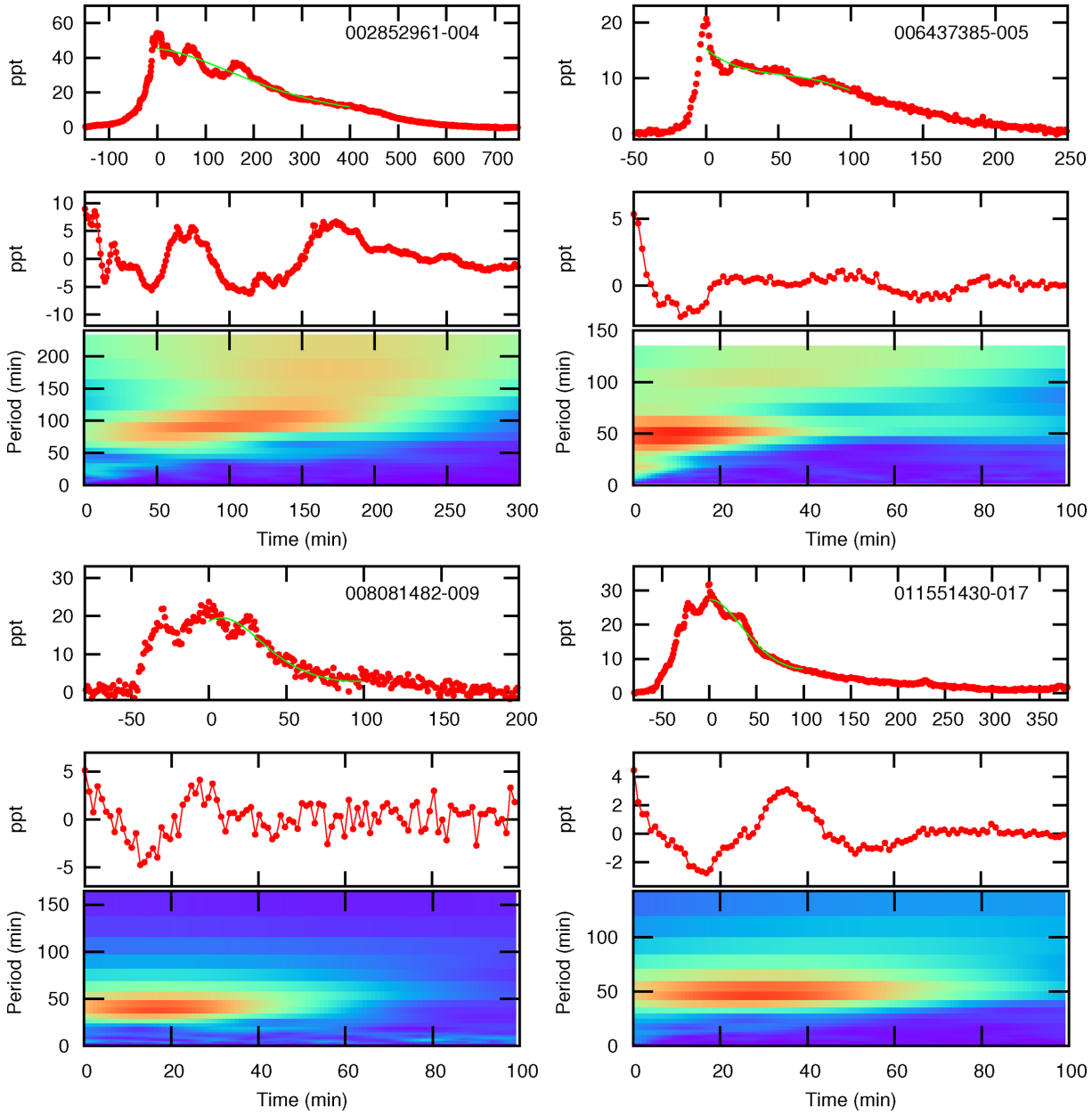

Figure 1. Examples of four flares showing bumps on the decay branch. The top panel shows the flare light curve and fitted polynomial. The middle panel shows the decay branch with polynomial removed, with time measured from the time of maximum flare intensity. The bottom panel shows the wavelet spectrum as a function of time relative to the time of maximum flare intensity. The intensity is measured in parts per thousand (ppt). The KIC number and the flare identifier from the catalogue of Balona (2015) is shown.

frequency needs to be taken into account in any analysis of significance. Because white noise is usually assumed the significance of QPP has generally been overestimated. This is further illustrated by recent work by Inglis, Ireland & Dominique (2015) who investigated supposed QPP in a selection of solar flares from a variety of sources as well as QPP in some optical stellar flares. They found that for all except one event tested, an explicit oscillation is not required in order to explain the observations. Instead, the flare signals are adequately described as a manifestation of a power law in the Fourier power spectrum, rather than a direct signature of oscillating components or structures.

That does not mean that all QPP signals are spurious, but that great caution needs to be exercised in determining the significance of QPP in flares. For this reason, we do not claim that the oscillating signals seen in Figs 2–8 are necessarily real. We merely wish to illustrate that QPP in the *Kepler* flares, if it exists, is not common.

While QPP is a useful diagnostic tool for flares on the Sun, it cannot be used for stellar flares without some underlying assumptions. In the Sun, one can image the flare, so that the loop length is known. Very often, other parameters, such as the plasma temperature, can also be quite well estimated. For stellar flares, however, we only have the period and decay time of the QPP, so the information that can be extracted is severely limited. Zaitsev & Stepanov (1982) and Roberts, Edwin & Benz (1984) showed that for a simple cylindrical magnetic flux tube, several types of magnetoacoustic wavemodes are possible: the slow (acoustic) mode, the fast kink and the fast sausage modes. These are all observed in solar flux tubes and solar

Table 1. Physical parameters for stars in which one or more bumps are visible in the flare light curve. The second column, N_f, is an identifier for the flare, which is the N_fth flare for the particular star in the catalogue of Balona (2015). The *Kepler* magnitude, *Kp*, effective temperature, $T_{\rm eff}$ (K) and surface gravity, $\log g$, is taken from the *Kepler Input Catalogue* (KIC). The luminosity, $L/{\rm L}_\odot$ is derived from the effective temperature and radius listed in the KIC. The average number of flares per day, N/d, and the total number of observed flares, N, are shown. The rotation period, $P_{\rm rot}$ (d), are from Balona (2015). $P_{\rm max}$ is the expected period of solar-like oscillations (min). The last column is the derived period from wavelet analysis.

KIC	N_f	Kp (K)	$T_{\rm eff}$ (dex)	$\log g$	$\log L/{\rm L}_\odot$	N/d	N (d)	$P_{\rm rot}$ (min)	$P_{\rm max}$ (min)	$P_{\rm bump}$
2300039	28	15.42	3644	4.294	− 0.9049	0.710	65	1.707	5.9	4.8
2852961	1	10.14	4722	2.877	1.3730	0.201	5	8.8:	175.9	80.6
–	3	–	–	–	–	–	–	–	–	68.0
–	4	–	–	–	–	–	–	–	–	97.0
4671547	59	11.29	4059	4.653	− 1.1032	2.453	64	8.138	2.7	12.5
–	62	–	–	–	–	–	–	–	–	7.0
5475645	3	11.20	5336	4.654	− 0.3709	0.059	6	7.452	3.1	9.2
5733906	2	11.83	5241	3.688	0.6933	0.238	7	0.719	28.6	5.5
5952403	2	6.96	5037	3.001	1.5178	0.012	2	45.28:	136.5	110.2
6205460	4	12.74	5242	3.677	0.7067	0.111	16	3.717	29.4	8.7
–	5	–	–	–	–	–	–	–	–	12.7
–	12	–	–	–	–	–	–	–	–	57.5
6437385	5	11.53	5401	3.713	0.7194	0.205	18	13.672	27.4	55.0
–	7	–	–	–	–	–	–	–	–	86.0
6548447	2	12.88	5031	4.005	0.2505	0.093	8	9.409	13.5	60.0
7885570	23	11.67	5398	4.616	− 0.3033	0.167	40	1.730	3.4	38.0
–	27	–	–	–	–	–	–	–	–	40.0
7940533	4	12.86	5326	4.555	− 0.2665	0.179	21	3.826	3.9	42.8
–	5	–	–	–	–	–	–	–	–	38.0
8081482	6	14.56	5522	4.333	0.0524	0.109	28	2.819	6.7	66.0
–	9	–	–	–	–	–	–	–	–	40.9
8226464	4	11.46	5754	4.053	0.4475	0.526	15	3.101	12.9	53.5
–	8	–	–	–	–	–	–	–	–	35.0
8608490	10	14.77	4897	3.955	0.2591	0.032	10	1.083	15.0	76.2
9349698	32	12.91	4911	4.537	− 0.4318	1.861	136	1.359	3.9	51.6
9576197	7	14.64	5082	4.551	− 0.3651	0.164	12	9.096	3.9	68.3
9641031	10	9.17	5867	4.295	0.2134	0.145	84	2.156	7.5	11.9
–	35	–	–	–	–	–	–	–	–	21.8
9655129	6	13.80	5140	4.431	− 0.2067	0.113	20	2.750	5.1	40.9
–	7	–	–	–	–	–	–	–	–	19.8
9833666	7	9.68	5411	3.735	0.6977	0.164	9	10.341	26.1	42.6
–	9	–	–	–	–	–	–	–	–	40.0
10063343	30	13.16	3976	4.433	− 0.8685	1.536	46	0.333	4.5	3.1
10976930	1	11.28	5934	3.644	0.9735	0.069	2	2.054	33.7	29.3
11445774	2	11.91	6108	4.328	0.2577	0.026	6	1.744	7.1	35.0
11551430	7	10.69	5335	3.729	0.6779	0.791	185	4.145	26.3	67.7
–	17	–	–	–	–	–	–	–	–	48.5
–	21	–	–	–	–	–	–	–	–	35.5
–	34	–	–	–	–	–	–	–	–	10.7
–	72	–	–	–	–	–	–	–	–	79.5
–	73	–	–	–	–	–	–	–	–	20.7
–	94	–	–	–	–	–	–	–	–	43.8
11610797	18	11.53	5865	4.464	0.0338	1.018	34	1.625	5.1	16.2
12156549	24	15.88	5541	4.378	0.0116	0.620	128	3.651	6.0	59.8

flare loops. For a standing oscillation in a loop, the loop length L is given by $L = jcP/2$, where P is the oscillation period, j the parallel mode number and c the appropriate wavespeed. The waves with the longest periods, which are those of interest to us due to the 1-min cadence of the *Kepler* data, are the slow modes. For slow modes, c is the tube speed, $c_{\rm t}$ with

$$\frac{1}{c_{\rm t}^2} = \frac{1}{c_{\rm s}^2} + \frac{1}{c_{\rm A}^2},$$

where $c_{\rm s}$ is the sound speed and $c_{\rm A}$ is the Alfvén speed. Since the Alfvén speed in the coronal loops is considerably larger than the sound speed, we assume $c \approx c_{\rm s}$.

The unknown values of j, c and L render the extraction of any meaningful physics impossible at this stage. We also note that the above description applies to a low-density plasma environment as occurs in a typical solar coronal flare loop. Stellar flares emit in a continuum and the physical process is likely to be different from that of solar flares even if the energy source, magnetic reconnection,

Table 2. Physical parameters for stars in which a damped oscillation (QPP) is visible in the flare light curve. The second column, N_f, is an identifier for the flare. The *Kepler* magnitude, *Kp*, effective temperature, $T_{\rm eff}$ (K) and surface gravity, $\log g$, is taken from the KIC. The average number of flares per day, N/d, and the total number of observed flares, N, are shown. The variability type and the rotation period, $P_{\rm rot}$ (d), are from Balona (2015). The last column is the period (min) derived from wavelet analysis.

KIC	N_f	Kp (K)	$T_{\rm eff}$ (dex)	$\log g$	N/d	N	$P_{\rm rot}$ (d)	$P_{\rm QPP}$ (min)
2300039	28	15.42	3644	4.294	0.710	65	1.707	4.8
3128488	17	11.66	4475	4.615	1.138	38	6.160	6.0
4671547	59	11.29	4059	4.653	2.453	64	8.138	6.0
–	62	–	–	–	–	–	–	5.0
11551430	21	10.69	5335	3.729	0.791	185	4.145	11.0
–	34	–	–	–	–	–	–	10.7
11610797	18	11.53	5865	4.464	1.018	34	1.625	14.0

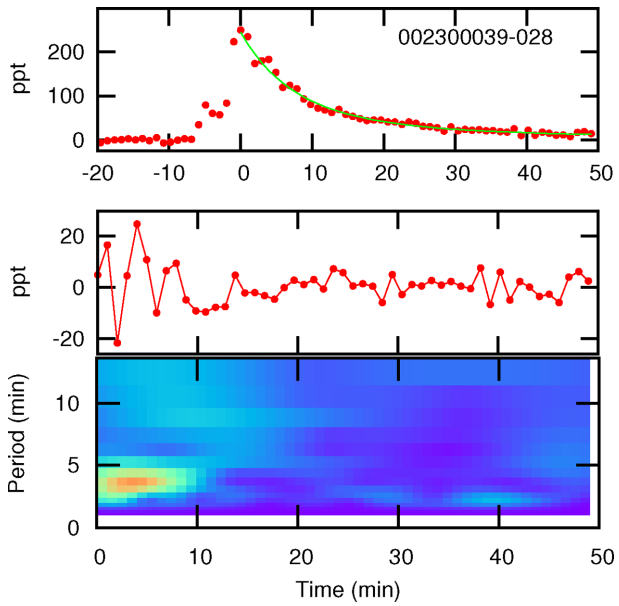

Figure 2. The top panel shows the flare light curve and fitted spline curve. The second panel shows the decay branch with fitted curve removed. The third panel shows the wavelet spectrum.

is the same. However, these parameters are contained in the characteristic parameters of the decay phase of the flare, the damping time of the oscillations, intensity of the flare and other observables and, in principle, can be extracted from the data when a sufficiently detailed model becomes available.

5 FLARES IN STARS WITH SOLAR-LIKE OSCILLATIONS

We know that some solar flares may excite local seismic disturbances (Kosovichev & Zharkova 1998; Kosovichev 2006), with maximum power in waves of high spherical harmonic degree, l. These waves would not be visible in whole-disc photometry because the net brightness change is cancelled owing to the small spatial wavelengths. The power in waves with low l which might be visible is very low (Kosovichev 2005). The more powerful impulse provided by a stellar superflare may, however, lead to observable results (starquakes). As described in the Introduction, the expected result is that the amplitudes of some global modes will grow while

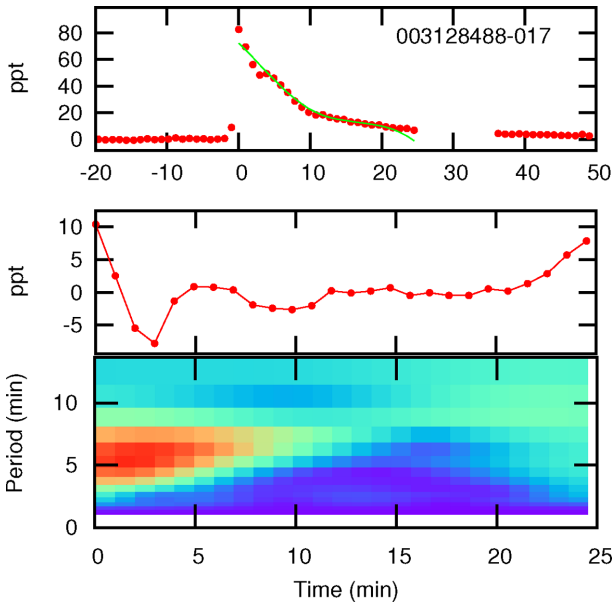

Figure 3. The same as Fig. 2.

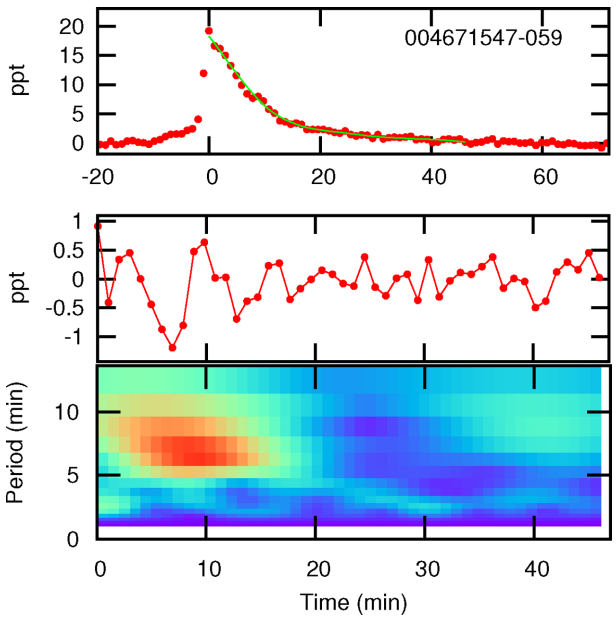

Figure 4. The same as Fig. 2.

others will diminish after a flare. It is therefore to be expected that the net result will be a larger variability of the energy in the global modes after the flare which can manifest itself as a larger variability in the periodogram.

The *Kepler* SC data are an ideal data set for studying possible starquakes. Among the 209 flare stars observed in SC mode, we can identify eight stars (Table 3) which clearly show the characteristic Gaussian envelope of solar-like oscillations in the periodogram. The relevant portion of the periodograms are shown in Fig. 9.

Karoff (2014) calculated the pre- and post-flare acoustic spectra from substrings of different lengths before and after the flares. The photometric variability associated with the flares was evaluated by measuring the total energy in the high-frequency part of both the pre- and post-flare acoustic spectra. Measuring the total power in a given frequency range may not be the most efficient method of

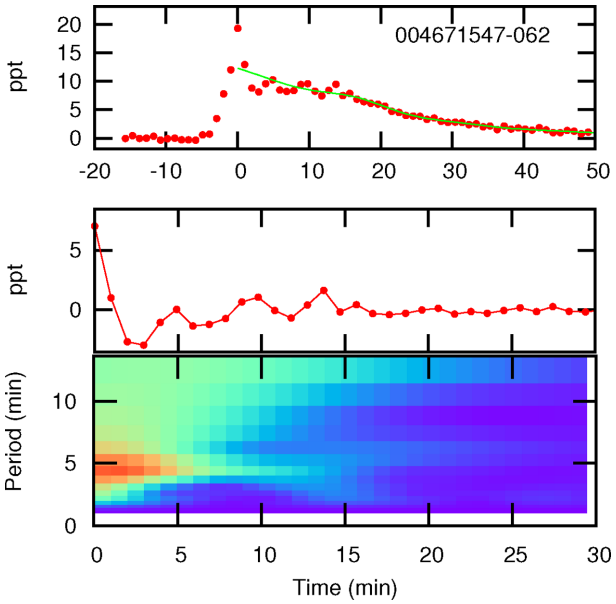

Figure 5. The same as Fig. 2.

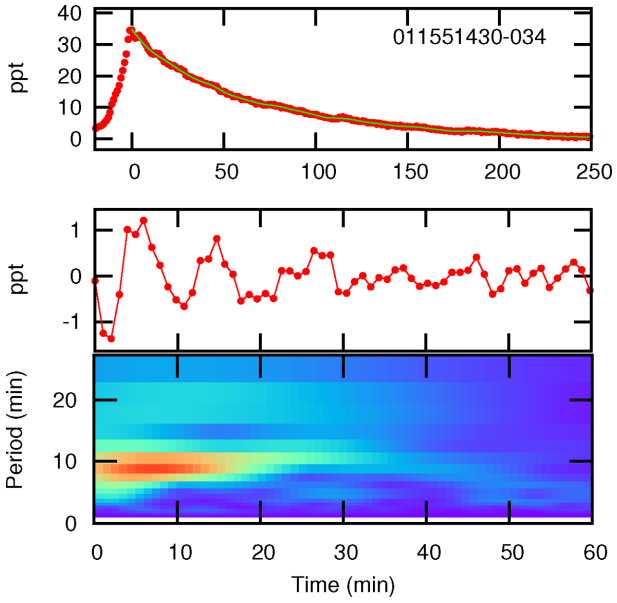

Figure 7. The same as Fig. 2.

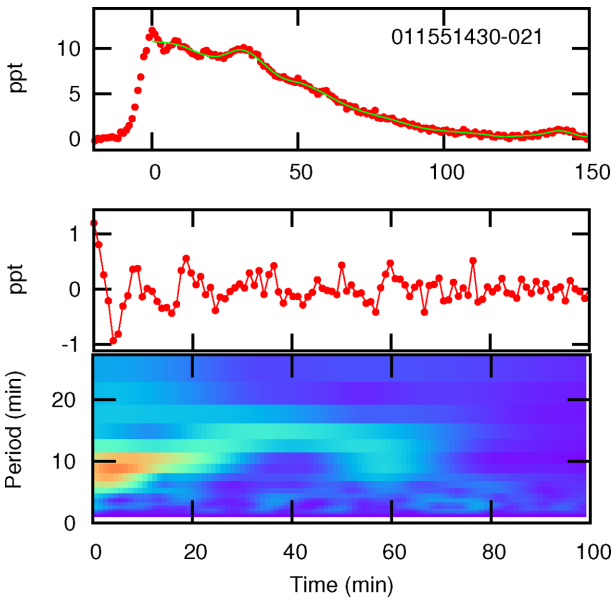

Figure 6. The same as Fig. 2.

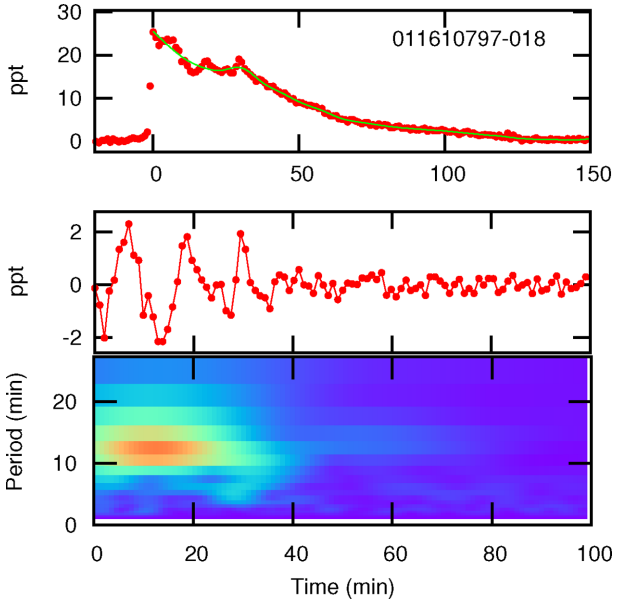

Figure 8. The same as Fig. 2.

Table 3. Parameters for flare stars with solar-like oscillations.

KIC	*Kp*	$T_{\rm eff}$ (K)	log *g* (dex)	log $L/L_\odot$	N/d	N	$P_{\rm rot}$ (d)
3430868	8.13	4729	4.584	−0.5864	0.203	6	–
4554830	10.33	5317	4.314	−0.0051	0.039	1	14.602
5108214	7.83	5663	3.857	0.6404	0.028	8	–
6442183	8.52	5760	4.006	0.4606	0.015	15	–
7206837	9.76	6100	4.148	0.4527	0.032	35	4.050
7940546	7.39	5987	4.170	0.3916	0.041	37	–
7944142	7.81	4630	2.796	1.3908	0.121	3	1.729
12307366	11.50	4958	3.654	0.6328	0.006	6	–

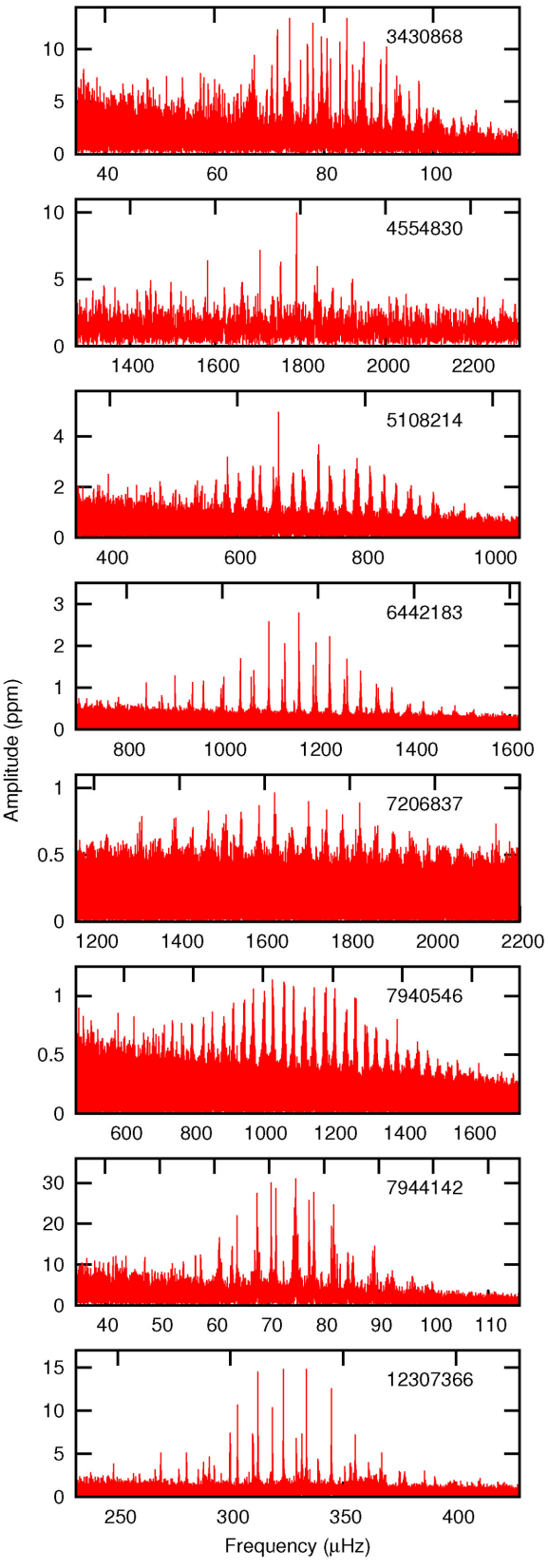

Figure 9. Periodograms of flare stars with solar-like oscillations.

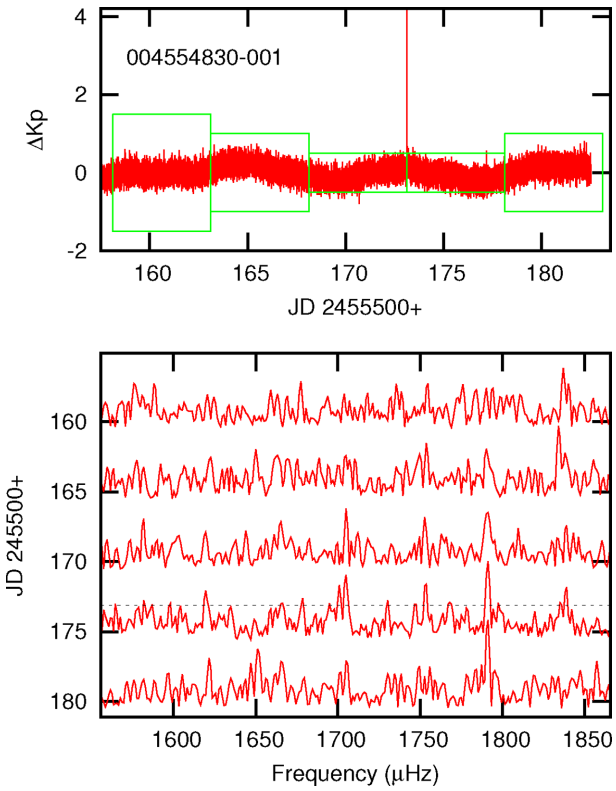

Figure 10. Top panel: light curve of KIC 4554830 showing flare and regions where periodograms were calculated. Bottom panel: periodograms of the regions shown in the top panel showing the solar-like oscillations. The dotted line shows the time of the flare.

detecting changes in the solar-like oscillations because the spectra are noise limited. In other words, a significant part of the total power comes from the noise and not the actual oscillations. Instead, it might be best to compare the amplitudes of individual peaks in the periodogram of the global oscillations before and after the flare. In this way one may hope to detect possible systematic increases or decreases of amplitude in individual modes as might be expected.

In Fig. 10, we show the light curve and periodogram of KIC 4554830 around the time of a flare. The periodogram is calculated using two or three 5-d data windows before and after the flare. Because of the stochastic nature of solar-like oscillations, changes in amplitude of individual peaks are to be expected. One therefore needs to examine several different frequency peaks and to determine if the changes in amplitude (increase or decrease) is significantly larger than would normally occur. In KIC 4554830, the amplitude of the mode at 1790.99 μHz appears to increase after the flare. On the other hand, the amplitude of the mode at 1839.41 μHz seems to decrease. The data windows are independent (no overlap) so one can judge the significance of the amplitude changes.

Similar diagrams may be created for all flare stars with solar-like oscillations, but this may not be the best method of detecting starquakes. Since we are looking for changes in amplitude of individual modes, we selected several peaks of large amplitude and fitted a truncated Fourier series to the data window using these frequencies. This gives us the amplitude and its standard deviation for each frequency peak. We performed this calculation in two data windows before and after the flare.

Fig. 11 shows the resulting amplitudes in each 5-d window as a function of time for all solar-like modes of sufficient amplitude.

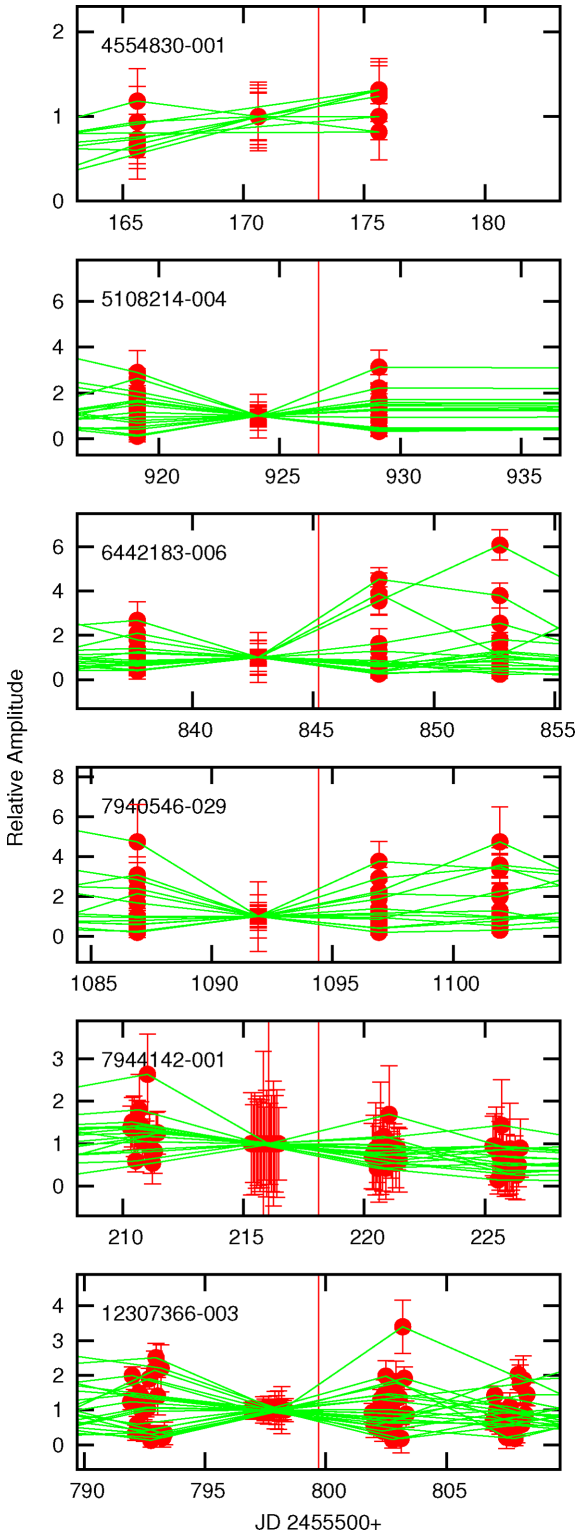

Figure 11. Pulsation amplitudes for solar-like oscillations as a function of time. The amplitudes have been normalized to the values just before the flare and 1σ error bars are shown. Solid lines join individual mode frequencies. The time of the flare is indicated by the vertical line.

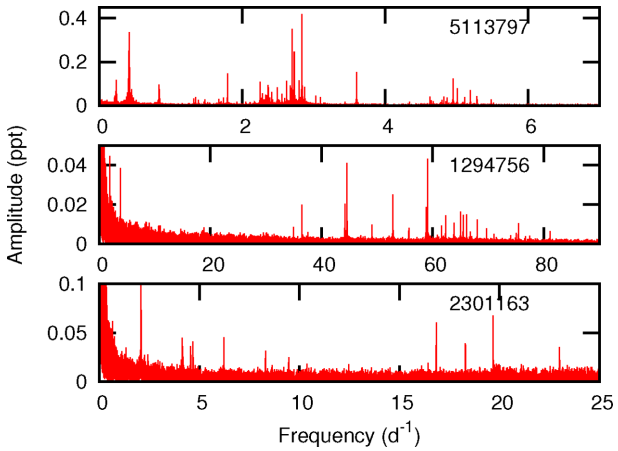

Figure 12. Periodograms of a γ Dor star (KIC 5113797, top panel) and two δ Sct stars that show flares.

For clarity, all amplitudes are normalized to their values in the window just before the flare. The same mode is connected with a solid line. Judging from the error bars, it is evident that in no case is there a clear amplitude change after the flare relative to the pre-flare amplitude. We conclude that a superflare has no systematic influence on the amplitudes of the solar-like oscillations detectable by this technique.

This does not mean that starquakes do not occur, of course. The impulse generated by a superflare is bound to cause acoustic disturbances which could affect the amplitudes of global modes. However, the small spatial scale (high azimuthal degree) of such oscillations lead to cancellation effects, resulting in whole-disc light variations that are too small to detect.

6 FLARES IN δ SCUTI AND γ DORADUS STARS

It is very difficult to detect flares in classical pulsating stars because the light variations due to the pulsation tend to mask short-lived rapid excursions such as a flare. This is especially true for short-period variables. Nevertheless, among the SC observations, flares are seen in the δ Sct stars KIC 1294756 and KIC 2301163. Both these stars have extremely low pulsation amplitudes, rendering the flares more easily visible. The flare star KIC 5113797 seems to be a γ Dor variable of low amplitude. The periodograms of these stars are shown in Fig. 12.

The oscillations in δ Sct and γ Dor stars are self-excited with reasonably stable amplitudes and phases, unlike the stochastic solar-like oscillations. Hence changes in pulsation amplitude after a flare might be easier to detect. Unfortunately, the S/N ratio in the δ Sct pulsations of KIC 2301163 is too low for the oscillations to be detected in a 5-d data window. Since the effect of a flare impulse on the oscillations is expected to dissipate rather quickly, one needs to use a short data window to optimize its detection. For this reason KIC 2301163 was excluded from the analysis. The low oscillation frequencies in the γ Dor variable KIC 5113797 means that very few pulsation cycles can be obtained during the 5-d window. As a result, the amplitudes and phases have large errors. This star, too, was omitted.

In Fig. 13, part of the light curve of the δ Sct star KIC 1294756 is shown centred on one of the flares. The boxes show the data windows used to construct the periodograms. Some amplitude changes seem to occur, particularly for the mode at 34.9317 d^{-1} which appears to decrease after the flare.

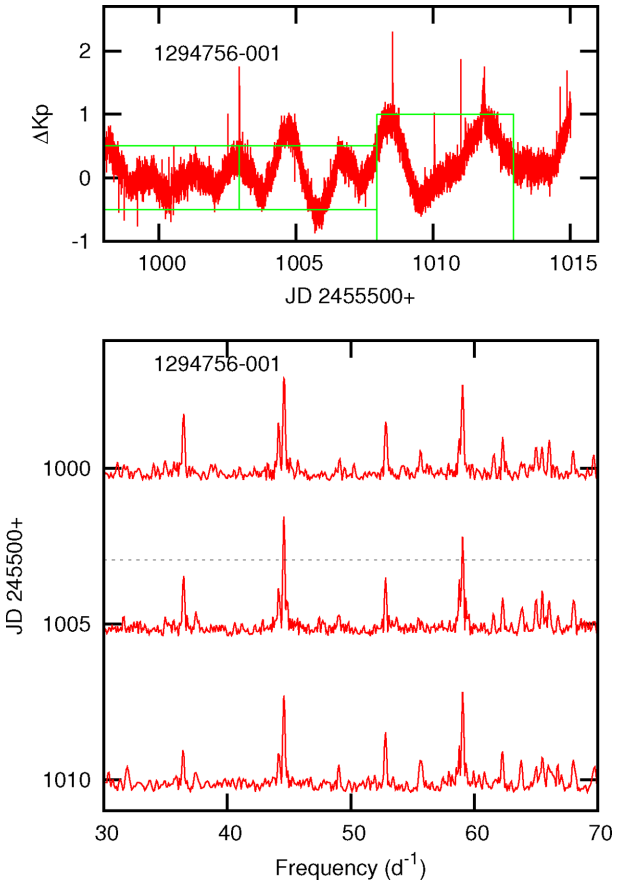

Figure 13. Top panel: light curve of the δ Sct star KIC 1294756 showing flare and regions where periodograms were calculated. Bottom panel: periodograms of the regions shown in the top panel showing the δ Sct pulsations.

In Fig. 14, we show how the pulsation amplitudes vary with time before and after the flare. In this figure, the data for two flares are shown. As before, the amplitudes are relative to the amplitudes just before the flare. Although there are variations in amplitude for many modes, these are within the expected errors and are therefore not significant. We conclude that even when the pulsation amplitudes are stable, there is no evidence that a flare affects the mode amplitudes in a manner that is detectable.

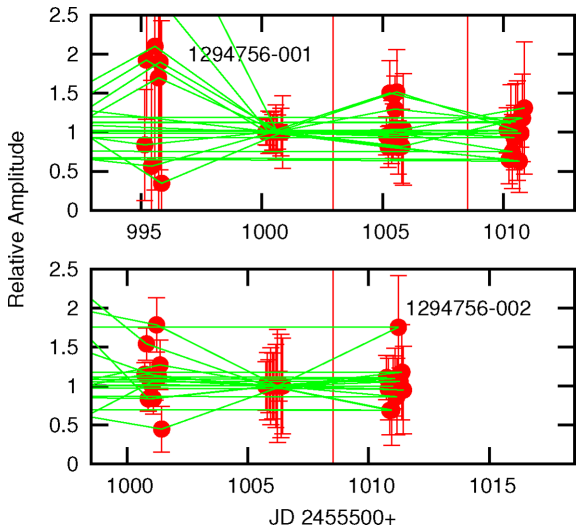

Figure 14. Relative pulsation amplitudes for the δ Sct star KIC 1294756 as a function of time. The amplitudes have been normalized to the values just before the flare and 1σ error bars are shown. The time of the flare is indicated by the vertical line.

7 CONCLUSION

In this paper, we investigate possible periodic light variations arising from stellar flares. By analogy to the Sun, QPP may be a result of MHD forces and other processes operating in the flare loop. These oscillations, which are often observed in solar flares, have also been detected in other stars and have periods in the range of seconds to tens of minutes. The period of the oscillation offers the potential to probe the magnetic field strength and temperature in the flare. However, nearly all the light in solar QPP is emitted in lines of highly ionized elements, whereas observations of stellar QPP are essentially white light. One cannot therefore directly compare solar and stellar QPP, though the underlying mechanism might still be the same.

QPP in some stellar flares observed from the ground (Rodono 1974; Zhilyaev et al. 2000; Mathioudakis et al. 2006; Contadakis et al. 2010; Qian et al. 2012) have been interpreted as analogous to flare QPP in the Sun, in spite of the very different light emission properties described above. These QPP generally have very short periods and last for several cycles. We searched for short-period QPP using wavelet analysis in all flares with high S/N and found seven flares in five stars in which such an oscillation seems to be present (Figs 2–8). The periods do not correlate with $\nu_{\rm max}$ or any stellar parameter. These are probably examples of the same phenomenon seen in the ground-based observations discussed above. They may not be directly comparable with QPP in solar flares, but perhaps a similar process may be active.

Oscillations in the light curve could also arise as a result of the impulse generated by a flare (a starquake). In the Sun, these are seen as surface waves of short spatial wavelength radiating from the location of the flare. There is evidence that the impact also affects the amplitudes of the stochastic global oscillations. For some modes a starquake will lead to an increase in amplitude, while for other modes a decrease in amplitude may be expected.

A significant fraction of stellar flares show clear structures (bumps) on the decaying branch of the light curve. We argue on probability grounds that these cannot be a result of almost simultaneous multiple flares. The bump may be modelled as rapidly decaying QPP. We tested the possibility that the bumps may be highly damped forced global oscillations by measuring the period using wavelet analysis. If these are forced global oscillations, one might expect the period to correlate with some stellar parameter. We could find no correlation with the estimated frequency of maximum amplitude, $\nu_{\rm max}$, resulting from solar-like oscillations or any other stellar parameter. We conclude that the bump cannot be understood as a forced global oscillation.

Finally, we attempted to detect forced global oscillations resulting from a starquake. These are expected to be visible shortly after a flare and are expected to modify the amplitudes of individual modes in stars where solar-like oscillations are detected. The best way to look for this effect is to measure the amplitudes of individual modes before and after a flare. There are eight stars in the *Kepler* SC observations which show flares and solar-like oscillations. Examination of the amplitudes of modes before and after a flare showed no obvious indication of significant amplitude changes. We conclude that the effect is too small to be detected in the *Kepler* data.

By their nature, random changes in amplitude are a characteristic of solar-like oscillations and this may mask an amplitude change resulting from a flare. The self-excited oscillations in δ Scuti and γ Doradus stars lead to generally stable amplitudes. Therefore, these stars may provide better detection of starquakes. We analysed the pulsation amplitudes of two δ Sct and one γ Dor star before and after a flare. Again, we were not able to find evidence of amplitude variations due to a flare.

A major problem in our understanding of stellar flares is that there are no corresponding observations in the Sun. Apart from the huge disparity in energy, solar flares emit almost entirely in emission lines of highly ionized elements whereas stellar flares are essentially white light flares. Furthermore, there are no reported observations of QPP in white-light solar flares. Such QPP may be detected in stellar flares observed in X-rays (Mitra-Kraev et al. 2005). The standard flare model suggests that the white-light emission in solar and stellar flares is triggered by non-thermal electrons which originate in the corona. There is a strong correspondence between white-light emission and hard X-ray emission (Hudson, Wolfson & Metcalf 2006). Moreover, solar hard X-ray bursts often show a high degree of periodicity (Aschwanden, Benz & Montello 1994). It is possible that the QPP seen in the few *Kepler* flares may be a result of these beams and their effect in the lower atmosphere. However, it may be difficult to understand white light flares in A stars where it is generally assumed that a corona is not present.

Our conclusion is that white-light QPP may possibly be seen in some *Kepler* flare stars, but their nature may differ from QPP in solar flares, although the processes involved could be similar. It would be important to synthesize whole-disc white light observations of solar flares. In this way we may hope to extend what we know of solar flares to stellar flares and thereby create a fuller understanding of the mechanisms involved in solar and stellar flares.

ACKNOWLEDGEMENTS

This paper includes data collected by the *Kepler* mission. Funding for the *Kepler* mission is provided by the NASA Science Mission directorate. The authors wish to thank the *Kepler* team for their generosity in allowing the data to be released and for their outstanding efforts which have made these results possible.

Much of the data presented in this paper were obtained from the Mikulski Archive for Space Telescopes (MAST). STScI is operated by the Association of Universities for Research in Astronomy, Inc., under NASA contract NAS5-26555. Support for MAST for non-HST data is provided by the NASA Office of Space Science via grant NNX09AF08G and by other grants and contracts.

LAB wishes to thank the South African Astronomical Observatory and the National Research Foundation for financial support. TV was sponsored by an Odysseus grant of the FWO Vlaanderen and performed in the context of the IAP P7/08 CHARM (Belspo) and the GOA-2015-014 (KU Leuven). This research was also sponsored by the European Research Council research project 321141 *SeismoSun* (CP, VMN) and STFC consolidated grant ST/L000733/1 (VMN). AGK thanks NASA for support (grant NNX14AB68G). AMB thanks the Institute of Advanced Study, University of Warwick for their financial support.

REFERENCES

Anfinogentov S., Nakariakov V. M., Mathioudakis M., Van Doorsselaere T., Kowalski A. F., 2013, ApJ, 773, 156
Aschwanden M. J., Benz A. O., Montello M. L., 1994, ApJ, 431, 432
Balona L. A., 2012, MNRAS, 423, 3420
Balona L. A., 2013, MNRAS, 431, 2240
Balona L. A., 2015, MNRAS, 447, 2714
Brown T. M., Gilliland R. L., Noyes R. W., Ramsey L. W., 1991, ApJ, 368, 599
Contadakis M. E., Avgoloupis S. J., Seiradakis J. H., 2010, in Tsinganos K., Hatzidimitriou D., Matsakos T., eds, ASP Conf. Ser. Vol. 424, Proceedings of the 9th International Conference of the Hellenic Astronomical Society. Astron. Soc. Pac., San Francisco, p. 189
Donea A.-C., Lindsey C., 2005, ApJ, 630, 1168
Donea A.-C., Braun D. C., Lindsey C., 1999, ApJ, 513, L143
Gruber D. et al., 2011, A&A, 533, A61
Hudson H. S., Wolfson C. J., Metcalf T. R., 2006, Sol. Phys., 234, 79
Inglis A. R., Ireland J., Dominique M., 2015, ApJ, 798, 108
Kane S. R., Kai K., Kosugi T., Enome S., Landecker P. B., McKenzie D. L., 1983, ApJ, 271, 376
Karoff C., 2014, ApJ, 781, L22
Karoff C., Kjeldsen H., 2008, ApJ, 678, L73
Kim S., Nakariakov V. M., Shibasaki K., 2012, ApJ, 756, L36
Kjeldsen H., Bedding T. R., 1995, A&A, 293, 87
Kosovichev A., 2005, AGU Fall Meeting Abstracts, A244, available at: http://saaoads.chpc.ac.za/abs/2005AGUFMSH11A0244K
Kosovichev A. G., 2006, Sol. Phys., 238, 1
Kosovichev A. G., 2009, in Guzik J. A., Bradley P. A., eds, AIP Conf. Proc. Vol. 1170, Stellar Pulsation: Challenges for Theory and Observation. Am. Inst. Phys., New York, p. 547
Kosovichev A. G., 2014, in Guzik J. A., Chaplin W. J., Handler G., Pigulski A., eds, Proc. IAU Symp. 301, Precision Asteroseismology. Cambridge Univ. Press, Cambridge, p. 349
Kosovichev A. G., Zharkova V. V., 1998, Nature, 393, 317
Kowalski A. F., Hawley S. L., Wisniewski J. P., Osten R. A., Hilton E. J., Holtzman J. A., Schmidt S. J., Davenport J. R. A., 2013, ApJS, 207, 15
Kretzschmar M., 2011, A&A, 530, A84
Kumar B., Mathur S., García R. A., Venkatakrishnan P., 2010, ApJ, 711, L12
Kupriyanova E. G., Melnikov V. F., Shibasaki K., 2013, Sol. Phys., 284, 559
McLaughlin J. A., Thurgood J. O., MacTaggart D., 2012, A&A, 548, A98
Maehara H. et al., 2012, Nature, 485, 478
Mathioudakis M., Seiradakis J. H., Williams D. R., Avgoloupis S., Bloomfield D. S., McAteer R. T. J., 2003, A&A, 403, 1101
Mathioudakis M., Bloomfield D. S., Jess D. B., Dhillon V. S., Marsh T. R., 2006, A&A, 456, 323
Mitra-Kraev U., Harra L. K., Williams D. R., Kraev E., 2005, A&A, 436, 1041
Moon Y.-J., Choe G. S., Park Y. D., Wang H., Gallagher P. T., Chae J., Yun H. S., Goode P. R., 2002, ApJ, 574, 434
Mullan D. J., MacDonald J., 2005, MNRAS, 356, 1139
Nakariakov V. M., Melnikov V. F., 2009, Space Sci. Rev., 149, 119
Nakariakov V. M., Inglis A. R., Zimovets I. V., Foullon C., Verwichte E., Sych R., Myagkova I. N., 2010, Plasma Phys. Control. Fusion, 52, 124009
Qian S.-B. et al., 2012, MNRAS, 423, 3646
Richardson M., Hill F., Stassun K. G., 2012, Sol. Phys., 281, 21
Roberts B., Edwin P. M., Benz A. O., 1984, ApJ, 279, 857
Rodono M., 1974, A&A, 32, 337
Shibata K. et al., 2013, PASJ, 65, 49
Shibayama T. et al., 2013, ApJS, 209, 5
Spruit H. C., 2002, A&A, 381, 923
Van Doorsselaere T., De Groof A., Zender J., Berghmans D., Goossens M., 2011, ApJ, 740, 90
Vaughan S., 2010, MNRAS, 402, 307
Walkowicz L. M. et al., 2011, AJ, 141, 50
Wang T., 2011, Space Sci. Rev., 158, 397
Zaitsev V. V., Stepanov A. V., 1982, Sov. Astron. Lett., 8, 132
Zhilyaev B. E. et al., 2000, A&A, 364, 641

This paper has been typeset from a TEX/LATEX file prepared by the author.